face of trypanosomes. Like the trypanosome surface membrane, the vacuolar membrane had underlying microtubules (Fig. 5F). The origin of these structures is unknown, but it may involve membrane transport or targeting.

The toxicity of O-11 for bloodstream trypanosomes may be related to the metabolism or function of the VSG GPI, especially because similar concentrations do not affect the growth and viability of procyclic trypanosomes. However, our experiments cannot rule out the possibility that toxicity is mediated by alteration of *N*-myristoylated proteins or by some change in membrane structure. The latter could be caused by incorporation of analog into phospholipids as well as into VSG. Whatever the mechanism of toxicity, these studies suggest a new approach to antitrypanosome chemotherapy.

REFERENCES AND NOTES

1. C. Laitman, *Trop. Dis. Res. News* **31**, 3 (1990).
2. S. L. Hajduk, P. T. Englund, D. H. Smith, in *Tropical and Geographic Medicine*, K. S. Warren and A. A. F. Mahmoud, Eds. (McGraw-Hill, New York, 1989), pp. 268–281; *Tropical Disease Research: Science at Work* (World Health Organization, Geneva, Switzerland, 1986).
3. G. A. M. Cross, *Annu. Rev. Cell Biol.* **6**, 1 (1990); T. L. Doering, W. J. Masterson, G. W. Hart, P. T. Englund, *J. Biol. Chem.* **265**, 611 (1990); M. G. Low and A. R. Saltiel, *Science* **239**, 268 (1988); J. R. Thomas, R. A. Dwek, T. W. Rademacher, *Biochemistry* **29**, 5413 (1990).
4. M. A. J. Ferguson and A. F. Williams, *Annu. Rev. Biochem.* **57**, 285 (1988).
5. M. A. J. Ferguson and G. A. M. Cross, *J. Biol. Chem.* **259**, 3011 (1984).
6. J. L. Krakow, D. Hereld, J. D. Bangs, G. W. Hart, P. T. Englund, *ibid.* **261**, 12147 (1986).
7. A. K. Menon, S. Mayor, M. A. J. Ferguson, M. Duszenko, G. A. M. Cross, *ibid.* **263**, 1970 (1988).
8. W. J. Masterson, T. L. Doering, G. W. Hart, P. T. Englund, *Cell* **56**, 793 (1989).
9. A. K. Menon, R. T. Schwarz, S. Mayor, G. A. M. Cross, *J. Biol. Chem.* **265**, 9033 (1990).
10. W. J. Masterson, J. Raper, T. L. Doering, G. W. Hart, P. T. Englund, *Cell* **62**, 73 (1990).
11. A. Mellors and A. Samad, *Parasitol. Today* **5**, 239 (1989).
12. H. Dixon, *Trans. R. Soc. Trop. Med. Hyg.* **61**, 12 (1967); D. M. Raben, unpublished observations.
13. R. O. Heuckeroth, L. Glaser, J. I. Gordon, *Proc. Natl. Acad. Sci. U.S.A.* **85**, 8795 (1988).
14. R. O. Heuckeroth and J. I. Gordon, *ibid.* **86**, 5262 (1989).
15. D. R. Johnson *et al.*, *ibid.* **87**, 8511 (1990).
16. J. L. Krakow, T. L. Doering, W. J. Masterson, G. W. Hart, P. T. Englund, *Mol. Biochem. Parasitol.* **36**, 263 (1989); S. Mayor *et al.*, *J. Biol. Chem.* **265**, 6164 (1990); S. Mayor, A. K. Menon, G. A. M. Cross, *ibid.*, p. 6174.
17. T. L. Doering, L. U. Buxbaum, J. Raper, unpublished observations.
18. The CoA derivative of O-11 (and of O-6 and O-13) is synthesized in the cell-free system as readily as that of myristate (*17*).
19. Glycolipid A and its [^{3}H]O-11–labeled counterpart are cleaved by PI-PLC from *Bacillus thuringiensis*, GPI-PLC from *T. brucei*, and GPI-PLD from human serum; glycolipid C and its counterpart only by GPI-PLD (PLC, phospholipase C; PLD, phospholipase D). Conditions were as in (*8*).
20. All analogs and myristate were adjusted to the same specific radioactivity throughout.
21. Mass analysis showed that after 6 hours of culture with 10 μM O-11 4% of the fatty acids on trypanosome VSG were O-11, affecting up to 8% of the VSG molecules (*17*).
22. M. L. Bryant, R. O. Heuckeroth, J. T. Kimata, L. Ratner, J. I. Gordon, *Proc. Natl. Acad. Sci. U.S.A.* **86**, 8655 (1989); M. L. Bryant *et al.*, *ibid.* **88**, 2055 (1991).
23. J. P. Richardson, R. P. Beecroft, D. L. Tolson, M. K. Liu, T. W. Pearson, *Mol. Biochem. Parasitol.* **31**, 203 (1988); C. E. Clayton and M. R. Mowatt, *J. Biol. Chem.* **264**, 15088 (1989).
24. Lysate preparation, washes, and incubation buffers as in (*10*).
25. J. D. Bangs, D. Hereld, J. L. Krakow, G. W. Hart, P. T. Englund, *Proc. Natl. Acad. Sci. U.S.A.* **82**, 3207 (1985).
26. T. L. Doering, W. J. Masterson, P. T. Englund, G. W. Hart, *J. Biol. Chem.* **264**, 11168 (1989).
27. Methanolysis of glycolipids A and C and examination of the resulting fatty acid methyl esters by reverse-phase thin layer chromatography showed that O-11 or myristate incorporated into these GPI species was not metabolized; similar analysis of the other (less polar) labeled lipids showed that they contained both unmodified [^{3}H]O-11 or [^{3}H]myristate as well as species that had been elongated (*17*).
28. B. Hamm, A. Schindler, D. Mecke, M. Duszenko, *Mol. Biochem. Parasitol.* **40**, 13 (1990).
29. I. Cunningham, *J. Protozool.* **24** (no. 2), 325 (1977).
30. G. A. M. Cross, *Parasitology* **71**, 393 (1975).

31. Supported by grants from the National Institutes of Health (AI21334 and AI27179), from the MacArthur Foundation, and from Monsanto Company. T.L.D. and L.U.B. are supported by Medical Scientist Training grant 5T32GM07309. We are grateful to J. Welply (Monsanto Corporation) for suggesting this collaboration. We appreciate M. Delannoy's help with the electron microscopy and T. Ting's and I. Chiu's assistance with phase microscopy. We thank V. Klein and S. Skiles for technical support; M. S. Pessin-Minsley and D. M. Raben for helpful advice; P. Talalay, T. A. B. Shapiro, and K. Mensa-Wilmot for reviewing this manuscript; and J. D. Bangs and W. J. Masterson for discussions. We thank G. A. M. Cross for providing *T. brucei* strain 427 (variant 221). We thank J. Eid and C. Decker for providing trypanosome strain TREU 667.

25 January 1991; accepted 9 May 1991

Reading a Neural Code

WILLIAM BIALEK,* FRED RIEKE,* ROB R. DE RUYTER VAN STEVENINCK,† DAVID WARLAND

Traditional approaches to neural coding characterize the encoding of known stimuli in average neural responses. Organisms face nearly the opposite task—extracting information about an unknown time-dependent stimulus from short segments of a spike train. Here the neural code was characterized from the point of view of the organism, culminating in algorithms for real-time stimulus estimation based on a single example of the spike train. These methods were applied to an identified movement-sensitive neuron in the fly visual system. Such decoding experiments determined the effective noise level and fault tolerance of neural computation, and the structure of the decoding algorithms suggested a simple model for real-time analog signal processing with spiking neurons.

ALL OF AN ORGANISM'S INFORMATION about the sensory world comes from real-time observation of the activity of its own neurons. Incoming sensory information is represented in sequences of essentially identical action potentials, or "spikes." To understand real-time signal processing in biological systems, one must first understand this representation: Does a single neuron signal only discrete stimulus "features," or can the spike train represent a continuous, time-varying input? How much information is carried by the spike train? Is the reliability of the encoded signal limited by noise at the sensory input or by noise and inefficiencies in the subsequent layers of neural processing? Is the neural code robust to errors in spike timing? Clear experimental answers to these questions have been elusive (*1, 2*). We present an approach to the characterization of the neural code that provides explicit and sometimes surprising answers to these questions.

The first recordings from single sensory neurons demonstrated that the intensity of a static stimulus can be coded in the firing rate of a sensory neuron (*3*). This concept of rate coding, extended to time-dependent stimuli, provides the framework for most studies of neural coding, leading to the definition of receptive fields, temporal filter characteristics, and so on. Beyond rate coding, a variety of different statistical measures have been proposed—interval distributions, correlation functions, and so forth (*1, 4*). As with the rate itself, these quantities can be seen as moments of the probability distribution $P[\{t_i\}|s(\tau)]$ that describes the likelihood of different spike trains $\{t_i\}$, given the stimulus $s(\tau)$ (*5*). These moments, however, are not properties of a single spike train; they are average properties of an ensemble of spike trains (*6*). Organisms rarely have the opportunity to compute these averages: To say that information is coded in firing rates is of no use to the organism unless one can

W. Bialek, F. Rieke, D. Warland, Department of Physics and Department of Molecular and Cell Biology, University of California, Berkeley, Berkeley, CA 94720.
R. R. de Ruyter van Steveninck, Department of Biophysics, Rijksuniversiteit Groningen, the Netherlands.

*Present address, NEC Research Institute, 4 Independence Way, Princeton, NJ 08540.
†Present address, Department of Audiology, University Hospital, P.O. Box 30.001, 9700 RB, Groningen, the Netherlands.

explain how the organism could estimate these firing rates from real-time observation of the spike trains of its own neurons (7).

The simplest problem of real-time signal processing is decoding the spike train to estimate the signal waveform. If one chooses an inappropriate definition of the signal this reconstruction will fail; for example, we have studied auditory neurons that provide enough information for reconstruction of the envelope of the acoustic stimulus but not of the waveform itself (8). One can define the signal encoded by a particular neuron to be that signal which is reconstructed most accurately from observation of the spike train. If one can reconstruct analog signals, then one can begin to understand how spike trains could be manipulated in subsequent stages of neural circuitry to perform more complex processing of these signals. It may not be possible, however, to interpolate between the discrete spikes to estimate a continuous stimulus.

The decoding problem is completely specified by the probability $P[s(\tau)|\{t_i\}]$ of a particular stimulus waveform $s(\tau)$ conditional on the spike train $\{t_i\}$. From this distribution, one can estimate the stimulus, for example, by finding the function of time that maximizes $P[s(\tau)|\{t_i\}]$. Thus, one approach to the decoding problem is to design experiments that directly measure $P[s(\tau)|\{t_i\}]$ (2). An alternative approach is to model the encoding process and analytically develop decoding algorithms within the context of the model; this approach (9) indicates that there is a broad regime in which linear filtering of the spike train results in an optimal estimate of the stimulus waveform (10). Are such simple decoding algorithms applicable to a real neuron?

The problem of reading the neural code is essentially the problem of building a (generally nonlinear) filter that operates continuously on the spike train to produce a real-time estimate of the unknown stimulus waveform (Fig. 1). If the spikes arrive at times $\{t_i\}$, our estimate of the signal is

$$s_{est}(t) = \sum_i F_1(t - t_i) + \sum_{i,j} F_2(t - t_i, t - t_j) + \ldots \quad (1)$$

To optimize the reconstructions one chooses the filters $\{F_n\}$ to minimize $\chi^2 = \int dt|s(t) - s_{est}(t)|^2$, where $s(t)$ is the true stimulus and the integration is over the duration of the experiment (11). The stimulus $s(t)$ is not restricted to simple sine waves or Gaussian noise, and thus one can study the coding of complex and naturalistic signals (8, 12). In this initial experiment, however, we used relatively simple stimuli.

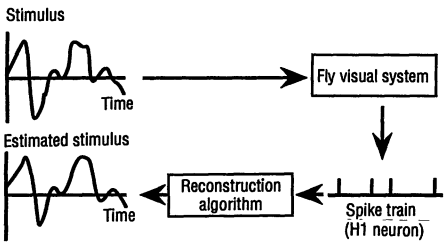

Fig. 1. Schematic view of the decoding process. The "black box" filters the spike train input $\{t_i\}$ to produce an estimate $s_{est}(\tau)$ of the stimulus.

We applied these ideas in experiments on a single, wide-field, movement-sensitive neuron (H1) in the visual system of the blowfly *Calliphora erythrocephela*. H1 encodes rigid horizontal movements over the entire visual field (13). Flies and other insects exhibit visually guided flight; during chasing behavior, course corrections can occur on time scales as short as 30 ms (14). The maximum firing rate in H1 is 100 to 200 s^{-1}, so behavioral decisions are based on just a few spikes from this neuron. Furthermore, the horizontal motion detection system consists of only a handful of cells, so the fly has no opportunity to compute average responses (for example, firing rates).

In our experiments, the stimulus $s(\tau)$ was the angular velocity of a rigidly moving random pattern. We chose $s(\tau)$ from an ensemble that approximated Gaussian noise with standard deviation 132 deg s^{-1}; the spectrum of $s(\tau)$ was constant up to a cutoff frequency of 1 kHz. We recorded the spike arrival times $\{t_i\}$ extracellularly from the H1 neuron (2, 15). We began by trying to reconstruct $s(\tau)$ with just the linear term of the general expansion, Eq. 1 (Fig. 2). Reconstructions including higher order terms in Eq. 1 were not significantly different, as quantified below. The filters used in the reconstruction integrated over short time intervals, so the optimal estimate of angular velocity at each instant of time was controlled by just a handful of spikes, as expected from behavioral studies.

How good are the reconstructions? The reconstructions consist of a piece that is deterministically related to the stimulus and a random noise piece. We separated these by introducing a frequency-dependent gain $g(\omega)$ such that $\tilde{s}_{est}(\omega) = g(\omega)\,[\tilde{s}(\omega) + \tilde{n}(\omega)]$, where $\tilde{n}(\omega)$ is the noise referred to the input. In a plot of $\tilde{s}(\omega)$ versus $\tilde{s}_{est}(\omega)$, the gain is the slope of the best linear fit and $\tilde{n}(\omega)$ is the scatter about this line. The distribution of $\tilde{n}(\omega)$ is approximately Gaussian.

Plotting the spectral density of the angular displacement noise, we found (Fig. 3) a peak signal-to-noise ratio (SNR) of better than 5:1, and an SNR of greater than one across a bandwidth of roughly 25 Hz. Using Shannon's formula (16), shown in Eq. 2, we converted these spectra into an estimate of the average rate at which we gained information about the stimulus (R_{info}) by virtue of observing the spike train; the result was 64 ± 1 bits per second (baud).

$$R_{info} = \int \frac{d\omega}{2\pi} \log_2\left[1 + \frac{\langle|\tilde{s}(\omega)|^2\rangle}{\langle|\tilde{n}(\omega)|^2\rangle}\right] \quad (2)$$

The second term in the expansion improved the information rate by less than 5%. We have not explored conditions that might maximize this information transmission.

The noise level achieved in the reconstructions is the noise against which an observer of the H1 spike trains (such as the fly) must discriminate to estimate horizontal motion.

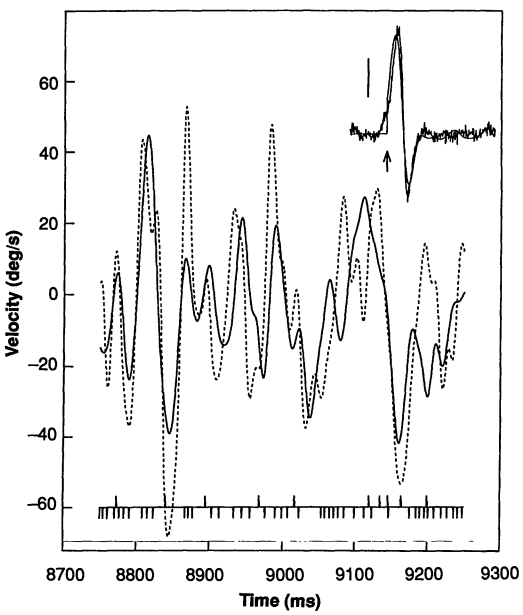

Fig. 2. First-order reconstruction (solid line) using method 1 (11). The stimulus is shown as a dotted line for comparison, and the spike train is shown at the bottom. This example is from a segment of the spike train that was not used in the filter calculations. Stimulus and reconstruction were smoothed with a 5-ms half-width Gaussian filter. (Inset) Filters calculated from methods 1 and 2 (11); the time scale is the same as the main figure, the scale bar = 10 deg s^{-1}, and the arrow marks $t = 0$. H1 has a highly asymmetric response profile, with a much larger dynamic range for movement in the excitatory direction. To compensate for this asymmetry, we recorded spike trains in response to $s(t)$ and to the inverted stimulus $-s(t)$; these are shown as positive and negative spikes in the spike train. These two spike trains approximate the trains that would be generated by H1 cells on opposite sides of the head during a rigid rotation of the fly (2). Our reconstruction is then

$$s_{est}(t) = \sum_i [F_1(t - t_i^+) - F_1(t - t_i^-)].$$

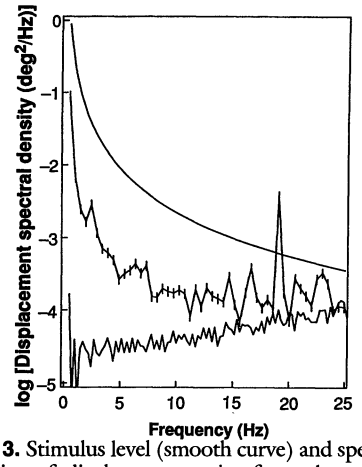

Fig. 3. Stimulus level (smooth curve) and spectral density of displacement noise from the reconstruction (middle curve). The bottom curve is the limit to the resolution of small displacements (valid for frequencies >10 Hz) set by noise in the photoreceptor array (*5*)

$$S_\theta^{\text{eff}}(\omega) = \frac{S_V(\omega)}{|\tilde{T}(\omega)|^2} \frac{32\pi^{1/2}}{NS_c} \frac{(\Delta\phi)^5}{\phi_0^2} \sinh[(1/2)(\phi_0/\Delta\phi)^2] \quad (4)$$

where S_c is the spectral density of the random contrast pattern used in the experiment, $\Delta\phi$ is the width of the photoreceptor aperture, ϕ_0 is the photoreceptor spacing along the direction of movement, $\tilde{T}(\omega)$ is the frequency response of the photoreceptor (millivolts per unit contrast), and $S_V(\omega)$ is the spectral density of voltage noise in the photoreceptor. The limiting noise power spectrum varies as the inverse of the number N of photoreceptors. These quantities were measured in photoreceptor recordings under conditions identical to those used for the H1 experiments (*15*), so we can make meaningful comparisons of theory and experiment.

The absolute noise level of the reconstructions is very low. With a behaviorally relevant integration time of 30 ms, one could judge the amplitude of a 20-Hz dither to within ~0.1 deg, which should be compared to the photoreceptor spacing of ϕ_0 = 1.35°. This angular resolution corresponds to the phenomenon of hyperacuity in human vision (*17*) and is in quantitative agreement with direct measures of discriminability for stepwise displacements in H1 (*15*). Defining an equivalent spectral density of noise in a spiking neuron allows one to exhibit hyperacuity in a real-time estimation task.

Information about movement across the visual field is carried in the spatiotemporal correlations of photoreceptor outputs, but these correlations are degraded by noise in the photoreceptors. How accurately can one estimate rigid motion if one optimally processes these noisy photoreceptor signals? In our stimulus ensemble, the angular displacements were small ($\delta\theta \ll \phi_0$) for frequencies above 10 Hz. In this limit, the optimal movement estimator involves multiplying the direct current voltage in one cell by the alternating current voltage in its nearest neighbor (*5*). This is essentially the "correlation" scheme for movement detection proposed by Reichardt (*18*); in our case, this algorithm was not a minimal model but rather the optimal computational strategy. Analysis of the correlation scheme (*5*) led to the limiting angular displacement noise level shown in Fig. 3, where the displacement noise from the linear reconstruction approaches the limits imposed by the photoreceptor noise, at least at frequencies above 10 Hz, where our theory of the limiting noise level is valid. The fly visual system thus performs an optimal and nearly noiseless extraction of movement signals from the array of photoreceptor voltages.

Coding is often used to reduce the effects of noise on signal transmission. Does the neural code have any such noise immunity? For several noise sources, such as timing errors, dropped spikes, and spontaneously generated spikes, we created an ensemble of spike trains which were randomly corrupted versions of the original data and then treated these as new data that required decoding. We were able to recover 95% of the original information R_{info} for the following noise levels: (i) spikes added to increase the firing rate by 20%, (ii) 5% of the spikes deleted, and (iii) Gaussian timing jitter with standard deviation of 2 ms introduced to each spike time. One objection to "spike timing" as a coding strategy is the need for precise measurement of spike arrival times. In the case of H1, this objection is irrelevant. The code is robust to errors of several milliseconds in spike timing and to other corruptions of the spike train..

Preliminary results from four studies suggest that linear decoding is not a special property of H1 under particular stimulus conditions but a more general property of sensory neurons.

1) In H1, we performed reconstruction experiments using stimuli with different spatial characteristics. These different stimulus ensembles provided different SNRs, and these differences were reflected in the reconstructions. Despite large changes in SNR, linear reconstruction continued to work and the reconstruction filters were essentially identical up to a constant scale factor.

2) In the mechanoreceptor cells of the cricket cercal system, the displacement waveform for motions of the filiform hairs was reconstructed from the spike trains of primary afferent neurons (*12*). For this system, the information transfer rates exceeded 300 baud (~3 bits per spike).

3) In simulations on realistic models (*19*) for spike initiation, we reconstructed the waveform of injected currents by linearly filtering the spike train.

4) In vibratory receptors of the bullfrog sacculus, we reconstructed the waveform of groundborne vibration using a linear decoding algorithm, although in this case the reconstructions improved substantially (by ~10 to 15%) with the addition of second-order terms (*8*). We again measured information rates close to 3 bits per spike.

It is, of course, not known if organisms perform the sort of reconstructions demonstrated in Fig. 2. Because linear reconstruction is possible, however, analog processing of the encoded signals can be done in a simple way. It is not unusual for the postsynaptic voltage response to a single presynaptic spike to have the qualitative form of the optimal filter, with a relatively sharp positive peak followed by a slower negative tail. Thus simple synapses could serve as decoders. With this decoding done, cells could then perform analog computations using the nonlinearities contributed by voltage-gated channels along the dendrites and cell body, much as envisioned for nonspiking cells (*20*). The results of such analog computations could then be encoded by the spike-generating region of the cell, and the process could then begin again. In this view of computation with spike trains, the combination of nonlinearities in spike generation and the filter characteristics of the synapse results in an essentially linear transmission of analog signals from presynaptic cell bodies to postsynaptic dendrites. The dramatic "all-or-none" nonlinearities of spike generation (the focus of so many models for neural computation) are then not as important as the more subtle analog dynamic properties of nonspiking regions of the cell.

It is surprising that time-dependent signals can be recovered so simply from neural spike trains. Reconstruction of the stimulus waveform permitted quantification of the fault tolerance of the code and allowed us to show that the fly visual system approaches optimal real-time computation. These results demonstrate that the representation of time-dependent sensory data in the nervous system is simpler than might have been expected. Correspondingly simpler models of sensory signal processing may be appropriate.

REFERENCES AND NOTES

1. D. Perkel and T. Bullock, *Neurosci. Res. Program Bull.* **6**, 221 (1968).
2. R. R. de Ruyter van Steveninck and W. Bialek, *Proc. R. Soc. London Ser. B* **234**, 379 (1988).
3. E. D. Adrian, *J. Physiol.* **61**, 47 (1926).
4. Recent work has focused attention on the time variation of firing rates in the auditory [for example, M. I. Miller, P. E. Bartaand, M. B. Sachs, *J. Acoust. Soc. Am.* **81**, 665 (1987)] and visual [for example, B. J. Richmond, L. M. Optican, H. Spitzer, *J. Neurophysiol* **64**, 351 (1990)] systems and on the

possible significance of temporal structure and correlated firing in the visual cortex [C. M. Gray and W. Singer, *Proc. Natl. Acad. Sci. U.S.A.* **86**, 1698 (1989)]. All these observations, however, involve measurements of average properties of spike trains over repeated presentations of a stimulus. Although these experiments are suggestive of coding strategies that different systems might use, none directly answers the question of how the organism could extract this coded information from single spike trains in real time.

5. W. Bialek, in *1989 Lectures in Complex Systems, SFI Studies in the Sciences of Complexity*, E. Jen, Ed. (Addison-Wesley, Reading, MA, 1990), vol. 2, pp. 513–595.
6. The most general of such approaches are the white-noise methods, such as reverse correlation [P. Marmarelis and V. Marmarelis, *Analysis of Physiological Systems. The White Noise Approach* (Plenum, New York, 1978)]. Although these methods do not rely on repeated presentation of identical stimuli, they nonetheless yield models that ideally predict the firing rate in response to arbitrarily chosen stimuli. Reverse correlation thus suffers the same limitations as other rate-based approaches.
7. Other authors have realized the importance of approaching neural coding from the point of view of the organism. In early work, R. Fitzhugh [*J. Gen. Physiol.* **41**, 675 (1958)] discusses real-time decision making. As far as we know, P. I. M. Johannesma [in G. Székely, E. Lábos, S. Damjanovich, Eds., *Adv. Physiol. Sci.* **30**, 103 (1981); Akadèmiai Kiadò, Budapest] comes closest to our approach.
8. F. Rieke, W. Yamada, K. Moortgat, E. R. Lewis, W. Bialek, in *Auditory Physiology and Perception: Proceedings of the 1991 European Hearing Workshop*, in press.
9. W. Bialek and A. Zee, *J. Stat. Phys.* **59**, 103 (1990).
10. Linear decoding might work for a trivial reason. Many sensory neurons have a regime in which the firing rate varies linearly with stimulus amplitude. This is an example of linear encoding and linear decoding might work as well in this regime. However, Bialek and Zee (*9*) predict that linear decoding is possible beyond the regime of linear input-output relations. The cell we studied in this work has a linear input-output regime, but the stimuli we used drove the cell outside this limit into saturation. See, for example, H. Eckert [*J. Comp. Physiol. A* **135**, 29, (1980)], who finds nonmonotonic rate-velocity profiles in the range of stimuli used here.
11. To ensure that the reconstruction process could be implemented in real time, we required that the filters be causal, for example, $F_1(\tau < 0) = 0$. We calculated the minimum χ^2 causal filters in two ways: (i) The best filter is first calculated without the causality constraint. An explicit formula can be written for this filter in terms of the spike trains and the stimulus

$$F_1(\tau) = \int \frac{d\omega}{2\pi} e^{-i\omega\tau} \frac{\left\langle \tilde{s}(\omega) \sum_j e^{-i\omega t_j} \right\rangle}{\left\langle \sum_{i,j} e^{i\omega(t_i - t_j)} \right\rangle} \quad (3)$$

where $\tilde{s}(\omega) = \langle d\tau \rightarrow \tilde{s}(\omega) = \int d\tau \rangle$. The averages (inside triangular brackets) are over the ensemble of stimuli $s(\tau)$ used in the experiment. This filter can be shifted by a delay τ_{delay} and causality can be imposed by setting the shifted filter to zero at negative times. (ii) χ^2 can be minimized with respect to purely causal functions by expansion of the filters $\{F_n\}$ in a complete set of functions that vanish at negative times. In this method, a delay time must be explicitly introduced that measures the lag between the true stimulus and the reconstruction, so $\chi^2(\tau_{delay}) = \int dt |s(t - \tau_{delay}) - s_{est}(t)|^2$ is minimized. These two methods together ensure that the optimal causal filters are calculated.
12. D. Warland, M. A. Landolfa, J. P. Miller, W. Bialek, in *Analysis and Modeling of Neural Systems*, F. Eeckman, Ed. (Kluwer, Norwell, MA, in press).
13. K. Hausen, in *Photoreception and Vision in Invertebrates*, M. Ali, Ed. (Plenum, New York, 1984).
14. M. Land and T. Collett, *J. Comp. Physiol.* **89**, 331 (1974).
15. R. R. de Ruyter van Steveninck, *Real-Time Performance of a Movement-Sensitive Neuron in the Blowfly Visual System* (Rijksuniversiteit Groningen, Groningen, the Netherlands, 1986).
16. C. Shannon, *Bell Syst. Tech. Jour.* **27**, 379 (1948).
17. G. Westheimer, *Invest. Ophthalmol.* **14**, 570 (1975).
18. W. Reichardt, in *Principles of Sensory Communication*, W. Rosenblith, Ed. (Wiley, New York, 1961).
19. C. Koch and I. Segev, Eds., *Methods in Neuronal Modeling* (MIT Press, Cambridge, MA, 1989).
20. C. Koch, T. Poggio, V. Torre, *Proc. Natl. Acad. Sci. U.S.A.*, **80**, 2799 (1983).
21. We thank W. J. Bruno, M. Crair, W. Gerstner, L. Kruglyak, J. P. Miller, W. G. Owen, A. Zee, and G. Zweig for helpful discussions and D. A. Baylor, D. Glaser, and M. Meister for thoughtful comments on the manuscript. Preliminary work on simulations of model neurons was done with L. Kruglyak, the results on the cricket cercal system were obtained in collaboration with M. A. Landolfa and J. P. Miller, and the experiments on the bullfrog auditory system were done in collaboration with W. Yamada and E. R. Lewis. Work at Berkeley was supported in part by the NSF through a Presidential Young Investigator Award to W.B., supplemented by funds from Cray Research, Sun Microsystems, and the NEC Research Institute, and through a Graduate Fellowship to F.R. D.W. was supported in part by the Systems and Integrative Biology Training Program of the NIH. Initial work was supported by the Netherlands Organization for Pure Scientific Research (ZWO). Research also performed at NEC Research Institute by W.B. and F.R.

2 November 1990; accepted 10 May 1991

Massive Cortical Reorganization After Sensory Deafferentation in Adult Macaques

TIM P. PONS,* PRESTON E. GARRAGHTY, ALEXANDER K. OMMAYA, JON H. KAAS, EDWARD TAUB, MORTIMER MISHKIN

After limited sensory deafferentations in adult primates, somatosensory cortical maps reorganize over a distance of 1 to 2 millimeters mediolaterally, that is, in the dimension along which different body parts are represented. This amount of reorganization was considered to be an upper limit imposed by the size of the projection zones of individual thalamocortical axons, which typically also extend a mediolateral distance of 1 to 2 millimeters. However, after extensive long-term deafferentations in adult primates, changes in cortical maps were found to be an order of magnitude greater than those previously described. These results show the need for a reevaluation of both the upper limit of cortical reorganization in adult primates and the mechanisms responsible for it.

MERZENICH AND HIS COLLEAGUES demonstrated that primary cortical sensory maps in adult animals, like those in infant animals, are capable of reorganization after various peripheral sensory perturbations (*1, 2*). Yet, compared to the massive functional changes that have been found in neonates, in which entire cortical maps may be reorganized (*3*), the changes reported in adults have been relatively small, with an upper limit of 1 to 2 mm along the cortical surface (*1, 2, 4*). Although the finding of any plasticity in primary sensory maps of adult animals was unexpected, the limited extent of the changes suggested they were confined to the projection zones of single thalamocortical axons (*1, 2*). Both the limits of reorganization and the mechanisms responsible must now be reconsidered because of new evidence in adult macaques showing reorganization in the cortex at least an order of magnitude greater than that reported previously.

Tactually elicited neuronal activity was recorded in area SI (*5*) of four cynomolgus monkeys (*Macaca fascicularis*) that had received deafferentations of an upper limb, three unilateral and one bilateral, more than 12 years before the recording session (*6*). All procedures were carried out in accordance with NIH guidelines on the care and use of laboratory animals (*7*). Electrode penetrations were placed approximately 0.75 mm apart across the mediolateral extent of the cortical region that had been deprived of its normal input and less densely in parts of the cortex containing maps of body parts that were unaffected by the deafferentation procedure. We typically recorded activity for each 300-μm advance of the electrode in a penetration.

Normally the cortical representations of body parts are organized into highly topographic maps (*8, 9*) (Fig. 1). In macaques, the upper limb representation in SI is always bordered by the representation of the trunk medially and the face laterally (*10*). In the region of the border of the face and hand representations, which is located opposite the tip of the intraparietal sulcus (*8*), the face map contains the representation of the chin

T. P. Pons, A. K. Ommaya, M. Mishkin, Laboratory of Neuropsychology, National Institute of Mental Health, Building 9, Room 1N107, Bethesda, MD 20892.
P. E. Garraghty and J. H. Kaas, Department of Psychology, Vanderbilt University, Nashville, TN 37240.
E. Taub, Department of Psychology, University of Alabama at Birmingham, Birmingham, AL 35294.

*To whom correspondence should be addressed.